ACES Asian Chemical Editorial Society

doi.org/10.1002/cnma.202300532

CHEMNANOMAT
Review

www.chemnanomat.org

Nanoparticle-Based Cryogels from Colloidal Aqueous Dispersion: Synthesis, Properties and Applications

Hadir Borg,[a, b, c] Irene Morales,[a, b, c] Dirk Dorfs,[b, c, d, e] and Nadja C. Bigall*[b, c, d, e]

Cryogels have morphological features that make them interesting for several applications such as catalysis, sensing or tissue engineering. Their interconnected network and open porous structure, build up by primary particles (such as inorganic nanocrystals or polymers), provide these materials with unique physical properties and high specific surface areas. While the library of cryogels is endless, widely used in the polymer chemistry field, in this review we will summarize the structure and properties, applications and challenges of inorganic nanocrystal-based cryogels obtained by freezing and freeze-drying an aqueous nanoparticle colloid. This fast, easy and versatile gelation method will be outlined, along with the corresponding macro-, micro- and nano-structures and gel morphologies that can be obtained, for example, by changing the freezing temperature or by using one nanoparticle system or nanoparticle mixtures. Their applications towards electrocatalysis, photocatalysis and photoelectrochemical sensing will be highlighted, as well as the challenges and prospects of these materials.

1. Introduction

The assembly of inorganic nanocrystal has attracted considerable attention in the last decades.[1–6] Although this assembly can give rise to ordered structures,[7,8] such as superlattices or mesocrystals, nonordered assemblies are receiving increased attention, and one of the most prominent and emergent examples of that are the inorganic nanocrystal-based gels. This special structuring of the matter gives rise to macroscopic materials with high specific surface areas and low densities that can retain the individual properties of the nanocrystals or showcase structure-dependent features arising from the interactions between the building blocks in the network and their spatial distribution.[3]

First of all, it is important to define what is a gel in general terms and what different kind of gels can be made. The International Union of Pure and Applied Chemistry (IUPAC) defines a gel as "non-fluid colloidal network or polymer network that is expanded throughout its whole volume by a fluid".[9] In addition to that, in the document it is specified that a gel can contain i) a polymer network formed through different processes: covalent polymer network by crosslinking polymer chains, physical aggregation of polymer chains, polymer network formed by glassy junction point …, ii) lamellar structures (e.g. soap gels, clays …) and/or iii) particulate disordered structures. Therefore, a gel consists on interconnected polymers or nanocrystals and a dispersed phase. This definition brings a starting point to join all the gel community under the same umbrella, which is a challenging task: the gel community is very broad and diverse due to the possibility of making gels out of virtually any kind of material.

Different terminologies are frequently used depending on the dispersed phase and on the applied drying technique. In general, when the interconnected network is embedded in a liquid, they are referred to as lyogels or solvogels. In particular, when the dispersed phase is water, they are frequently called hydrogels or aquagels, and the term alcogels is used when the dispersed phase is an alcohol or a mixture of them. As well, terms as lipogels and oleogels can be found in the literature, being gels where the dispersed phase is a nonpolar organic solvent. Finally, when the dispersed phase is air, they are known as aerogels.

Aerogels can be obtained by different drying techniques such as supercritical drying, freeze-drying, microwave drying, or vacuum drying of hydrogels.[10] The main challenge is to replace the solvent from the pores of the network with air preventing the collapse of the structure and for that, it is necessary to circumvent the capillary forces and high surface tensions in the

[a] H. Borg, Dr. I. Morales
Institute of Physical Chemistry and Electrochemistry
Leibniz University Hannover
Callinstraße 3a, 30167 Hannover, Germany

[b] H. Borg, Dr. I. Morales, Prof. Dr. D. Dorfs, Prof. Dr. N. C. Bigall
Cluster of Excellence, PhoenixD
(Photonics, Optics, and Engineering – Innovation Across Disciplines)
Leibniz University Hannover
30167 Hannover, Germany

[c] H. Borg, Dr. I. Morales, Prof. Dr. D. Dorfs, Prof. Dr. N. C. Bigall
Laboratory for Nano and Quantum Engineering
Leibniz University Hannover
30167 Hannover, Germany

[d] Prof. Dr. D. Dorfs, Prof. Dr. N. C. Bigall
Institute of Physical Chemistry
University of Hamburg
Grindelallee 117, 20146 Hamburg, Germany
E-mail: nadja-carola.bigall@uni-hamburg.de

[e] Prof. Dr. D. Dorfs, Prof. Dr. N. C. Bigall
The Hamburg Centre for Ultrafast Imaging
University of Hamburg
Hamburg, Germany

liquid-gas interface. The first aerogel, which was a silica aerogel, was fabricated by Kistler in 1931[11] as a bet of whether it was possible to replace all the liquid of a jelly by air without changing the overall volume. Kistler proposed a brilliant method, which is still widely used nowadays with some modifications, known as supercritical drying (SCD). By using an autoclave and increasing the pressure and the temperature above the critical temperature of the solvent of the gel, a supercritical fluid is obtained, which is afterwards allowed to escape slowly by decreasing the pressure at constant temperature, leaving the internal network of the gel intact. Despite their unique properties and potential, aerogel research was left aside during several decades after its discovery due to the complicated, expensive and hazardous fabrication method. In 1985, a novel, cheaper and less dangerous technique was proposed to supercritically dry gels by substituting the solvent within the gel with liquid CO_2, which allowed to reduce the temperature from more than 270 °C to less than 40 °C, as well as the pressure and the drying time.[12] The aerogels obtained by supercritical drying are referred directly as aerogels. If the drying of the solvent is done by simple evaporation and under ambient conditions, the resulting gel is called Xerogel. In this case, the capillary forces in the interface of the solvent and the network cause a significant shrinkage of the structure, which could be reduced by using a solvent with a lower surface tension.

Apart from supercritical drying, the second most extended drying technique is called freeze-drying or lyophilization, which consists first on the freezing of the solvent (normally water) followed by the sublimation of the ice crystals, giving place to what is known as cryoaerogels.

In general, a cryogel is a type of gel which is fabricated at sub-zero temperatures[13–16]. Basically, cryogels can be understood as hydrogels in which the polymerization or the gelation happens at temperatures below zero, giving place to highly porous interconnected networks. When the ice crystals are removed from the network by sublimation by means of a freeze-dryer, the resulting structure is called cryoaerogel (the pores are now filled with air).[16] If the cryogel is then presented in its wet form, it should be referred to as cryohydrogel.

The cryogelation technique was developed in 1970[17] and it has been widely used with polymeric materials, such as acrylate,

Hadir Borg was born in Mansoura in 1993. She got her B.Sc. in Pharmaceutical Sciences in 2014 and then her M.Ss. in Pharmaceutical Sciences (Analytical Chemistry) in 2017 from Mansoura University. From 2014 to 2021, she was doing research focused on pharmaceutical analysis at Delta University for Science and Technology. Since 2021 until now, she is doing her PhD degree at Leibniz Univertsität Hannover in the research group of Prof. Dorfs and Prof. Bigall. Currently, her research interest are the synthesis and characterization of noble metal nanoparticles-based cryogels and their applications.

Irene Morales was born in Madrid in 1991. She got her B.Sc. in Physics in 2015 and M.Sc. in Nanophysics and Advanced Materials in 2016 from the University Complutense of Madrid. She obtained her PhD in Physics at the Institute of Applied Magnetism-University Complutense of Madrid in 2021. Since 2022, she is a postdoctoral researcher in the group of Prof. Bigall at Leibniz Universität Hannover (LUH) and in 2023 she got the Caroline Herschel fellowship granted by the LUH. Her research interests include the synthesis, characterization and applications of multifunctional magnetic nanocrystal assemblies.

Dirk Dorfs studied chemistry at the University of Hamburg and obtained a PhD degree from the Technical University of Dresden (group of Alexander Eychmüller). He worked as a postdoc at the Hebrew University of Jerusalem (group of Uri Banin) and subsequently at the Italian Institute of Technology (group of Liberato Manna). From 2011 to 2023 Dirk Dorfs worked as a researcher at the Leibniz University of Hannover where he holds the position of extraordinary Professor since 2019. Since 2024 he has joined Hamburg University as a research group leader. Dirk Dorfs is interested in synthesis and shape control of nanocrystals and multi-component nanocrystals and in the investigation of alternative plasmonic materials.

Nadja C. Bigall was born in Munich in 1979. She graduated in physics at Ludwig Maximilians Universität in 2005 followed by a doctorate at TU Dresden in 2009 in physical chemistry. After postdoctoral work at the Italian Institute of Technology and at Philipps-Universität Marburg, she built up her research group at Leibniz Universität Hannover, where she became an associate professor in 2017 and full professor in 2018. Since 2024 she is full professor at Universität Hamburg. Her research interests are the synthesis, characterization, and structure-property correlation of functional nanostructures, such as colloidal nanocrystals and assemblies thereof.

alginate, chitosan, and cellulose[18–20], among others. It is a very versatile, easy, inexpensive and fast technique, and that is the reason why it has flourished as a perfect route to produce inorganic nanoparticle-based cryogels. To draw one example, for applications in the field of electro- or photocatalysis, it is possible to easily fabricate noble metal nanoparticle-based cryogels in the form of thin films with high specific surface areas and an open porous structure (catalysts), regardless of the size, shape or surface functionalization of the building blocks. Moreover, their performance is better than for the non cryogelated counterpart (the colloidal solution).[21]

In this review we will focus on the fabrication, structure, properties and applications of nanocrystal-based cryogels (either cryoaerogels or cryohydrogels), mainly fabricated directly from the aqueous nanoparticle solution and we will highlight the current challenges and prospects of this materials.

2. Fabrication and Macro-Structuring

This versatile technique is based on the freezing and subsequent solvent crystal evaporation of a gelling solution, which can be polymeric precursors,[22] a mixture of polymer/nanoparticles dispersed in an aqueous solvent,[23,24] a nanoparticle colloid, or a preformed hydrogel.[25,26] The principle of cryogelation is based on the occurrence of a heterophase system at low temperatures, which consists of a solid phase (the ice crystals of the solvent) and another unfrozen liquid microphase (in between the ice crystals) that contains the gelling solutes (Figure 1a).[17] The gelation step can only occur in this liquid microphase. In this context, gelation means crosslinking of the solvent precursors, which can happen by either a covalent linkage (chemically linked cryogel) or noncovalent linkage (physically linked cryogel).

The first studies on cryogels focused on the fabrication of polymer-based gels. The fabrication involves mainly the following steps: 1) phase separation (which happens upon formation of the ice crystals), 2) cross linking of the monomers, 3) polymerization and 4) thawing or freeze drying to get the highly porous interconnected network structure as a (cryo)hydrogel or a (cryo)aerogel, respectively.[27] Fabrication of polymer based gels via cryogelation has several advantages including the simplicity of the preparation steps and the suitability for various biological applications due to the useof aqueous solvents.[28] As the ice crystals solid-phase act as the template for shaping the cryogel microstructure, it is possible to tune the porosity of the structure by changing the freezing temperature and/or the type of the aqueous solvent. In polymer-based cryogels, it is also possible to control the elasticity of the cryogel material, for example, by changing the polymer concentration and the ratio of the cross-linker. This allows to engineer liver tissue models that mimics different physiological states of the liver.[29] Other possible applications of biocompatible polymer-based cryogels in tissue engineering and tissue regeneration have been previously illustrated in many reports.[30–33]

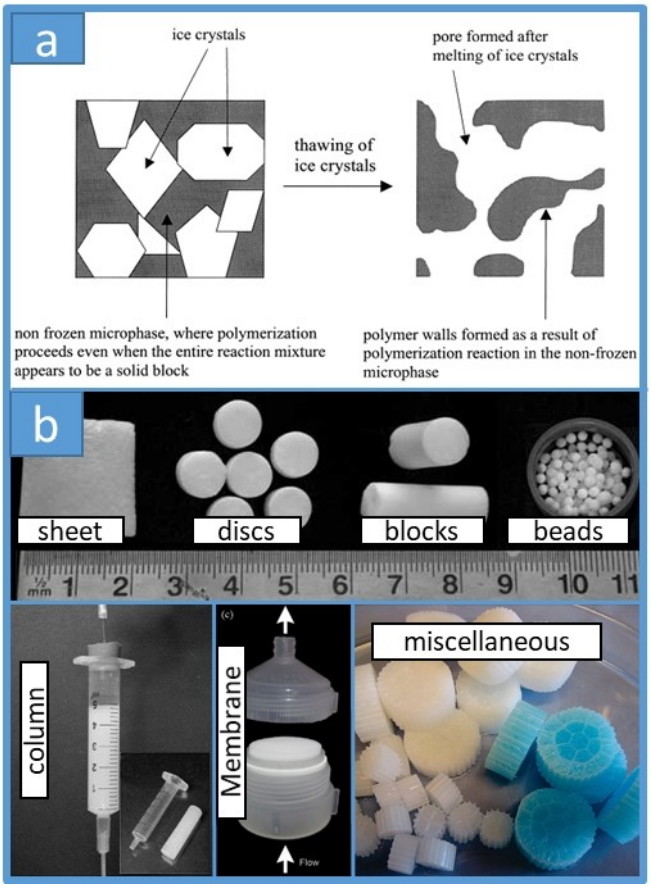

Figure 1. a) Schematic illustration of the polymerization process during cryogelation.[88] Adapted with permission.[88] Copyright © 2002 Elsevier Science B.V. All rights reserved. b) Different geometric shapes of polymer based cryogels, they can be fabricated either in the form of sheet, discs, blocks, beads,[89] columns,[90] membrane,[91] or any other miscellaneous shapes using plastic Kaldnes as carriers.[92] Adapted with permission[89]. Copyright © 2011 WILEY-VCH Verlag GmbH & Co. KGaA, Weinheim. Adapted with permission.[90] Copyright © 2002 Published by Elsevier B.V. Adapted with permission.[91] Copyright © 2012 Elsevier B.V. All rights reserved. Adpted with permission.[92] Copyright © 2008, American Chemical Society.

Several years later, fabrication of polymer based cryogels was extended to involve the addition of inorganic nanocrystals. Several works on cryogels obtained from mixing polymeric matrices with various types of nanoparticles have been reported including Ag,[23,24,34–47] Au,[48–54] Pd,[55,56] Pt,[55,56] Co,[57–63] Ni,[59–64] Cu,[60–62,64,65] Fe_3O_4,[66–71] ZnO,[72,73] SiO_2,[74] AlO_3,[75] SnO_2,[76] On one hand, the presence of the polymer matrix gives the cryogel material some features including: elastic texture, high water retention capacity and biocompatibility.[16,77] On the other hand, incorporation of inorganic nanoparticles adds other physical and chemical properties to the cryogel structure and allows the preparation of thermo-responsive, fluorescent, conductive and magnetic cryogels, for example.[78–81]

Polymer based cryogels can be fabricated in many shapes like sheets, discs, monoliths, columns, beads and membranes (Figure 1b), which makes it easy to adapt cryogels in different applications from the fabrication point of view. The work on polymer based cryogels is vast and many reviews have

summarized the previous studies and their possible applications.[16,22,28,77,82] All of these studies paved the way to the works in 2014 and 2016 of cryogels from inorganic nanocrystals in aqueous solutions, which is the main focus of this review.[83,84]

The cryogelation by freezing and freeze-drying directly of an aqueous nanocrystal solution is thoroughly investigated by our group[84–87] obtaining self-supported porous networks from different nanoparticle systems, i.e. Au, Ag, Pd, Pt, hematite Fe_2O_3, and CdSe/CdS rods, with densities ranging from 20–60 mg/cm^3 (around 0.2% of the density of the bulk materials). Among the advantages there are the fast and easy preparation method, without chemical selectivity, no need of previous hydrogelation and it can be used for any nanoparticle system as long as it is in water and with a nanoparticle concentration (nanoparticle volume fraction) of at least 0.1%, otherwise the structure collapses and shrinks.

For the cryoaerogelation, the colloidal nanocrystal is flash-frozen into the freezing media, occurring a sudden and uniform crystallization. The ice crystallites act as a template, pushing the nanoparticles together in the space between them while they grow, resulting in an interconnected macroporous nanoparticle network. After that, the ice crystals are removed by sublimation to avoid capillary forces and therefore to prevent the collapse of the structure. This process is also known as lyophilization or freeze-drying.

Nevertheless, other cryogelation methods of inorganic nanoparticle colloids have been investigated as well. For example, noble metal aqueous colloids of Au, Ag, Pt and Pd NPs were previously gelated using relatively high salt concentrations (~10^2 mM) followed by freeze drying, obtaining noble metal cryoaerogels.[93,94]

To gain a deeper understanding of the other gelation mechanisms for nanoparticle-based aerogels, many useful reviews are available in literature, for example.[1,7,95–99] In general, the main differences between cryogelation and classical gelation techniques are the driving force for inducing gelation and the drying mechanism which will be discussed in the following section.

It is possible to have the final cryogels in the form of homogeneous thin films on conductive substrates or in the form of three-dimensional monoliths. To fabricate nanoparticle-based cryogel films, either from the aqueous nanoparticle colloid or the hydrogel, different possibilities are available, such as dip coating, doctor blade[100] casting or drop casting[101] (Figure 2a), after which the substrate and the sample is flash-frozen. This is interesting for many applications in which an electric contact is necessary between the gel and conductive substrates, being the electrode fabrication technique very easy and manageable, giving place to thin and homogeneous cryogel films in the order of a few nanometres.

By drop casting the nanoparticle solution without any binding additive (gelation agent) in a substrate before freezing, it is possible to distribute better the nanoparticles and the resulting films present a continuous network with the nanoparticles having direct contact between them. As it has been reported,[14] by this procedure the accessible surface is maximized compared to coatings where the drop casted solution includes the gelating agent. This is because, in the latter case, the deposition of the slurry mixture in a substrate leads to the breaking down of the network into smaller segments and therefore the coating has a loss of structure and the hierarchical pore is damaged, reducing the accessible surface area.

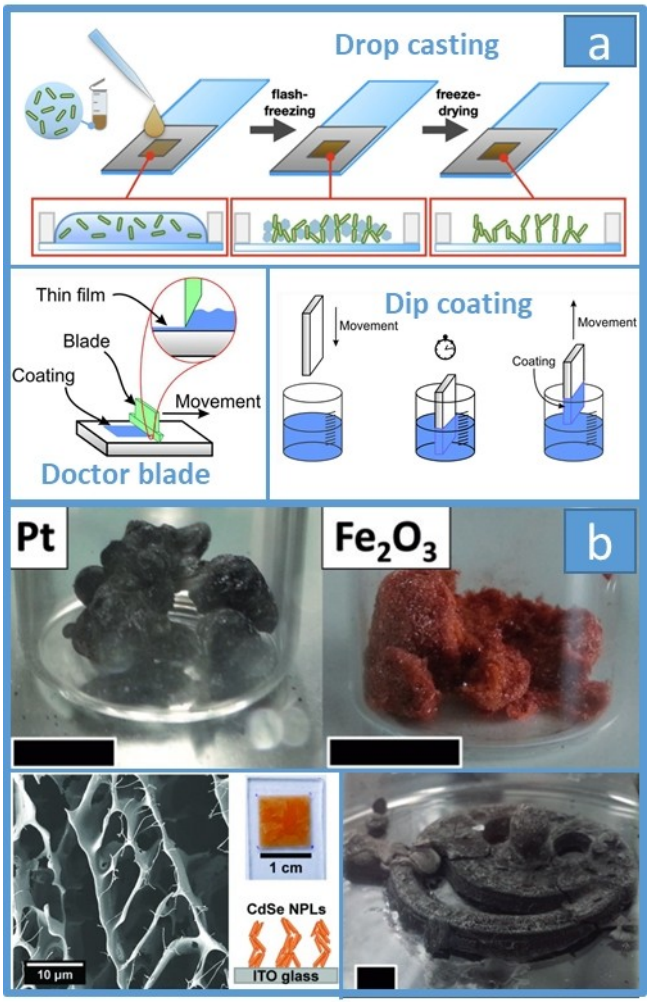

Figure 2. a) Schematic representation of nanocrystal-based cryogel film preparation: drop casting the nanoparticle solution in the film and subsequent flash freezing and freeze-drying[102], doctor blade and dip coating technique.[101] Adapted with permission[102].Copyright 2022 The Authors. Adapted with permission[101]. Copyright 2021 Springer Nature. b) Examples of the different cryoaerogels that can be obtained, either in the form of monoliths or molded monoliths[84] or films.[103] Adapted with permission[84]. Copyright 2016 Wiley-VCH. Adapted with permission.[103] Copyright 2019 The Royal Society of Chemistry.

As well, three-dimensional macroscopic materials can be obtained by means of cryogelation of inorganic nanoparticles. These sponge-like ultralight macroscopic materials are frequently referred to as monoliths (Figure 2b). For that, a drop of the aqueous nanoparticle colloid (various volumes can be used) is injected into the freezing media (e.g., liquid nitrogen) with the subsequent ice sublimation. Interestingly, these monoliths can be shaped into the desired form (Figure 2b). For that, the nanoparticles are included into a specific mold before freezing the solution and further freeze-drying. By the molding approach

it is therefore possible to shape the gel macroscopically, which could be interesting for several applications.[84]

Cryoprinting is an emerging technique, which has proven its interest to fabricate cryogels out of polymers, allowing to print a variety of shapes and sizes.[104] In this case, the solution was previously frozen and therefore the ice crystals were formed before printing. Afterwards, at −20 °C the polymer cryogel was photopolymerized into complex patterns using light-based printing technology. As well, in the case of the 3D printing of a chitosan cryogel, the authors used polyurethane nanoparticles as crosslinker at 4 °C during 4 h to obtain what they called a "pre-cryogel" and then it was extruded and deposited onto the printing platform at freezing temperatures (−20 °C).[105] As well, in this work[106], the authors created cryogel-based scaffolds out of gelatin by using an embedded 3D printing method for tissue engineering application. This method involves the gelation of the printed 3D structure at subzero temperatures under UV light. All this examples highlight and open very interesting possibilities for the printing of nanoparticle-based cryogels, in particular following the steps of the pioneer work done in our group,[107] using a commercial printer to simultaneously print nanoparticles and their destabilization agent to end up with aerogel printed films.

Finally, the main parameters which have an impact in the final internal structure and pore size of the cryogels during the cryogelation fabrication process are: i) the freezing media (e.g. liquid nitrogen vs. isopentane), ii) the temperature and iii) freezing rate.[14] In the fabrication of polymeric cryogels, it has been shown that the freezing temperature has an impact in the final pore size and shape of the freeze-dried cryogels, having open porous structures when the freezing temperature is between −20 °C to −80 °C, and parallel sheet structures when the temperature is lower (−196 °C).[16,108] The impact of these parameters in the structure and properties of inorganic nanoparticle-based cryogels will be discussed in detail in the next section.

3. Structure and Properties of Nanoparticles Based Cryogels

3.1. Morphology (Macroscopic, Microscopic and Nanoscopic)

Cryogels from colloidal NPs are interesting in regards to their morphological characteristics, regardless the type (Au, Ag, Pt, Pd, Fe_2O_3 or CdSe/CdS), shape (spherical, rods or nanoplatelets) or the size of the NPs building blocks (3.5–120 nm), the aerogels prepared by cryogelation method have common structural features.[84,102,103,109] In general, the cryogel monoliths look like fluffy chunks which are very brittle and easily breakable upon touching (Figure 2b and Figure 3a). This macroscopic shape can be easily modified by molding the aqueous NPs colloidal solution and obtain various macroscopic forms, like for example thin films (Figure 2b).

The colour of the cryoaerogel monoliths differ according to the properties of the NPs building the structure, for example, cryoaerogels from bare Ag NPs showed a reddish to violet colour, while Ag NPs covered with 5 and 12 nm silica shell resulted in green greyish and yellow brownish cryoaerogels, respectively (Figure 3a).[100] Cryoaerogels prepared from mixing different types of NPs also showed different colours according to the type and ratios of the NPs.[21]

Microscopically, the cryogel structure was found to mainly consist of extremely thin 2D sheet-like structures (ranging between 10–100 nm in thickness) which are randomly connected to form a 3D highly porous scaffold (Figure 3b).[110] These sheets are formed in the vicinities between the ice crystallites as a result of exclusion of the NPs from the colloid aqueous solution upon flash freezing at the cryogenic temperatures.

Therefore, the 2D sheets are consisting of the nanocrystals aligned together having inter-particle spaces in between. Generally, the particles are not fused together but they are very close on the atomic scale to allow charge carrier movement along the structure (Figure 3c).[86,87] This is highly interesting because the macroscopic structure of the cryogels can still retain the nanoscopic properties of the NPs. The 3D self-supporting structure is highly porous with large surface to volume ratio, the pores are formed in between the NPs within the 2D sheets (nanopores) and in between the 2D sheets (micropores) (Figure 3d and 3e),[87] the overall scaffold can be described as a sponge like voluminous structure. The porosity of the Ag/silica cryoaerogels were found to be 99.7 %.[100] The densities were found to range between 20–60 mg/cm^{-3} which represent only around 0.2 % of the corresponding bulk material.[110]

The concentration of the colloidal NPs solution used for cryogelation is critical. On one hand, if the NPs concentration is too low, the interconnection between the particles in the sheets will be poor resulting in a fragile structure with insufficient mechanical stability. Moreover, a shrinkage in the volume of the cryogel compared to the volume of the colloidal NPs solution is observed.

On the other hand, if the NPs concentration is increased (more than 0.1 vol %), the interconnection between the NPs in the sheets becomes better resulting in more rigid self-supported cryogel structures with no shrinkage in the volume of the cryogel compared to the volume of the colloidal NPs solution.[113] The thickness of the 2D sheets is found to increase along with increasing the NPs concentrations.

In order to compare the structure of nanoparticle-based cryogel material to other gels prepared by the classical gelation techniques, it is important to have a deep understanding of the differences in the gelation mechanisms. In the classical gelation techniques, gelation is induced through a controlled destabilization of the NPs colloidal dispersion. In this step, an external trigger is applied to reduce the repulsive forces between the NPs, which can be chemical or photochemical oxidation, heating, connecting functional groups of the ligands or changing in the zeta potential or the solvent polarity.[1] As an example, Figure 4a shows photographs for the gelation of CdSe quantum dots, triggered by chemical oxidation of the mercaptoundecanoic acid (MUA) by tetranitromethane as oxidizing

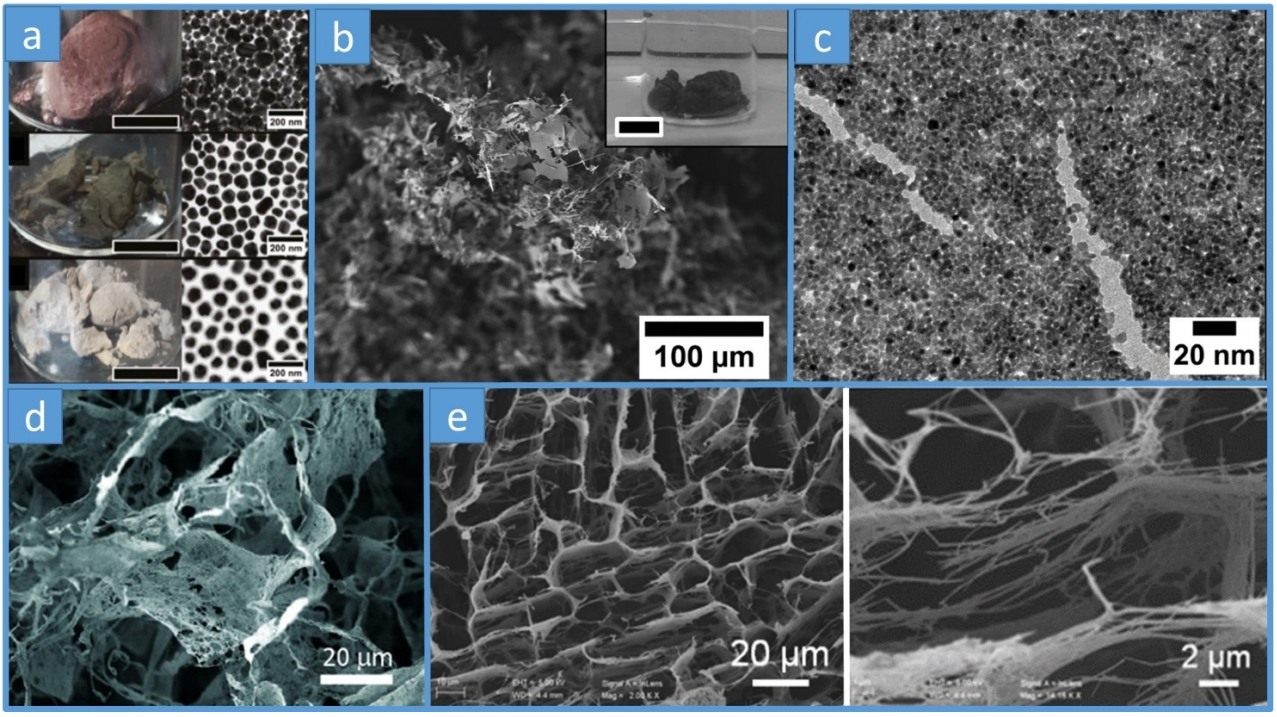

Figure 3. a) Cryoaerogel monoliths showing different colours according to the properties of the NPs building blocks [Top reddish to violet (bare Ag NPs), middle green greyish (Ag NPs with 5 nm silica shell), down yellow brownish (Ag NPs with 12 nm silica shell)] and their corresponding TEM images.[100] Adapted with permission[100].Copyright ©2018, Dirk Dorfs and Nadja Carola Bigall *et al.*, published by De Gruyter, Berlin/Boston. b) SEM image of cryoaerogel monolith made from Pt NPs showing the interconnection of the sheet like structures and the highly porous 3D scaffold. The inset shows a photographic image of the same Pt cryoaerogel monolith prepared from 1 mL of colloidal Pt NPs dispersion (Pt concentration: 0.025 %).[110]. Adapted with permission[110]. Copyright 2016 De Gruyter. c) TEM image of Pt cryoaerogel monolith sheet showing inter-particle spaces at the nanoscale.[110]. Adapted with permission[110]. Copyright 2016 De Gruyter. d) SEM image of cryoaerogel monolith made from Au nanowires showing the large pores (10–100 µm) formed due to the interconnection of the 2D sheet structures.[111]. Adapted with permission[111]. Copyright 2019 American Chemical Society. e) SEM images (top view) at different magnifications of cryoaerogel monoliths made from Ag nanowires showing the interconnection of the 2D network forming micropores.[112]. Adapted with permission.[112]. Copyright 2014 WILEY-VCH Verlag GmbH & Co. KGaA, Weinheim.

agent.[99] A well-defined gel structure can be seen at the bottom of the tube after aging time of 3 months. This gelation step is considered a crucial point since it influences the physical properties of the resulting colloidal network (e.g., porosity, density, mechanical stability and specific surface area). Instead, for cryogels, the gelation step is induced by freezing at cryogenic temperatures. So, the first difference between cryogelation and classical gelation methods is the driving force for inducing the gelation.

The gelation step is usually followed by a drying process, ideally the volume of the dried gel should be the same as the original wet gel. If the gel is dried under ambient conditions, a xerogel will be formed as shown in Figure 4b (left) which shrinks in size compared to the wet gel due to the capillary forces. On the other hand, if the gel is dried by supercritical drying as shown in Figure 4b (right), no shrinkage in the aerogel is observed compared to the wet gel. However, preserving the gel size in self-supported nanocrystal-based gels is not always guaranteed by supercritical drying as it can be influenced by the colloid concentration and the interparticle attraction forces. In comparison, cryogelation followed by freeze drying can to a large extend avoid this shrinkage problem.[113]

The microstructure of xerogels, aerogels and cryogels are very different, as shown from the SEM images in Figure 3 and 4c. The NPs in the xerogel structure are more compacted together than in the aerogel showing less porosity. On the other hand, the aerogel shows a highly porous structure. In both cases, the structure is completely different than the sheet-like structure obtained by cryoaerogelation. This feature is also visible at the nanoscale, as the TEM image of the aerogel in Figure 4(d–e) shows the connected filament-like structure which is again different than the cryoaerogel sheet-like feature (as previously shown in Figure 3c).

3.2. Composition (Pure and Mixed Nanocrystals)

Cryoaerogel monoliths from colloidal NPs, when firstly reported in 2016, were made from pure Au, Ag, Pt, Pd and Fe_2O_3 NPs and CdSe/CdS nanorods.[84] Surprisingly, there was almost no difference in the structure and morphology of the cryoaerogels formed from different types of NPs. In the same study it was proven that using different ligands on the surface of the Pt NPs (citrate, thioglycolic acid and mercaptosuccinic acid) also did not change the structure of the cryoaerogels. In later studies, cryoaerogels formed from pure Au, Ag, Pt and Pd showed the same typical structure and morphology of cryogels which

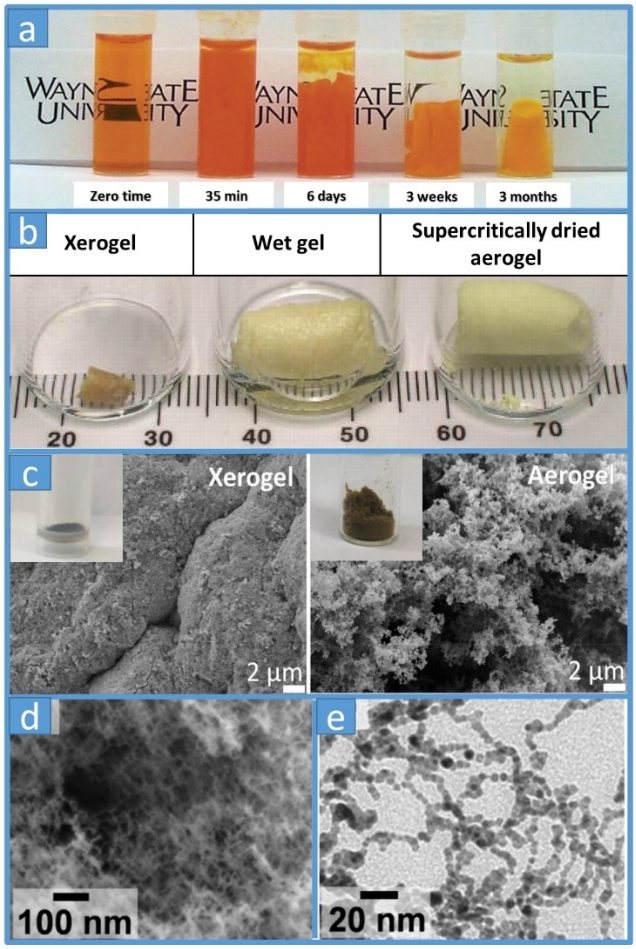

Figure 4. a) Photographs showing gelation of CdSe quantum dots over time after addition of gelating agent (oxidant: tetranitromethane).[99] Adapted with permission[99]. Copyright © 2007 American Chemical Society. b) A photograph compares the macroscopic characteristics of a wet CdS gel (middle) to the corresponding xerogel (left) dried under ambient conditions and the aerogel (right) dried by supercritical drying.[114] Adapted with permission[114]. Copyright © 2005, The American Association for the Advancement of Science. c) SEM images of $CuGaS_2$ nanocrystal-based xerogel (left) and aerogel after supercritical drying (right). Inset shows photographs of the corresponding sample.[115] Adapted with permission[115] © 2018 by the authors. Licensee MDPI, Basel, Switzerland. d) SEM and e) TEM images of aerogel from Pt/Ag NPs.[116] Adapted with permission.[116] Copyright © 2009 WILEY-VCH Verlag GmbH & Co. KGaA, Weinheim.

consists of randomly oriented 2D sheets which are further connected to form the 3D porous structure.[85,109]

Multicomponent cryogels can be obtained by mixing aqueous colloidal solution of different types of NPs followed by freezing (Figure 5a).[21,86,87] The advantage of mixing multiple types of NPs in the same cryogel structure is to obtain novel materials with improved properties. For example, Pt, Au or Ag were mixed with metal oxides and Au or Ag were mixed with hematite to obtain multicomponent cryoaerogel monoliths (Table 1).[21]

In other example, cryogel thin films were prepared from Au NPs mixed with CdSe/CdS nanorods or grown on it as a hybrid NPs. Similarly, Pt NPs mixed with CdSe/CdS nanoplatelets or grown on its edges as a hybrid NPs (Figure 5b).[86] Moreover, cryoaerogels from mixed Pt or Pd with Υ-Fe_2O_3 NPs were prepared as thin films supported on conductive ITO/glass substrates (Figure 5a).[87]

It is challenging yet important to obtain multicomponent cryogels with homogenous distribution of the NPs throughout the gel structure. The arrangement of the NPs within the multicomponent cryogel can be influenced by the ζ-potential of the NPs in the aqueous colloidal solution. It is well known that the electrostatic repulsion resulted from the same surface charge is important for a monodisperse colloidal NPs solution to keep the NPs stable and prevent aggregation. But what will happen when mixing different types of NPs colloidal solutions of opposite or the same surface charge? It was found that in the case of mixing NPs of different sizes, if the NPs have the same surface charge, this leads to local segregation.[21] In contrary, mixing NPs of different sizes and opposite surface charge leads to homogenous distribution in the cryogel structure.[21,87] The TEM images in Figure 5c showcase the influence of the surface charge of the NPs on the final homogeneity of the multicomponent cryogel structures.

3.3. Temperature Dependence

Freezing at cryogenic temperatures is a crucial point in cryogelation of NPs since the freezing speed is high enough to exclude the NPs in between the ice crystallites to form the 2D sheets. On the other hand, if the freezing speed is low, the NPs will be located within the ice crystallites and the cryogel network will not form.[14] It was also found that different freezing temperatures extremely influence the network structure of the cryoaerogels.[14] As mentioned before, during freezing, the NPs are excluded in the spaces between the ice crystals, and the cryogel network is templated according to the voids shaped between the ice crystals (Figure 6a). Therefore, the shape of the network was found to change between lamellar, cellular and dendritic according to the freezing temperature, which can be controlled by using different freezing media. This structural diversity of the cryoaerogel thin films was investigated by Müller *et al.*[14] in 2021 for different freezing temperatures and freezing media. In this study, it was shown that freezing the sample in liquid nitrogen (at 77 K) leads to a decrease in the freezing speed due to the Leidenfrost effect. To avoid this phenomenon and to obtain higher freezing speeds, different non-polar solvents were used at their melting point as a freezing media. This allowed freezing the samples at 179, 178, 142 and 113 K using n-hexane, toluene, n-pentane and isopentane, respectively. Increased freezing rate at low temperatures not only affected the network structure but also enhanced stability of the gel network (Figure 6b–e).

3.4. Interparticle Distance

The interaction between the particles in the initial aqueous colloidal solution is highly important and it finally affects the structure of the cryogel formed. An excellent example is the

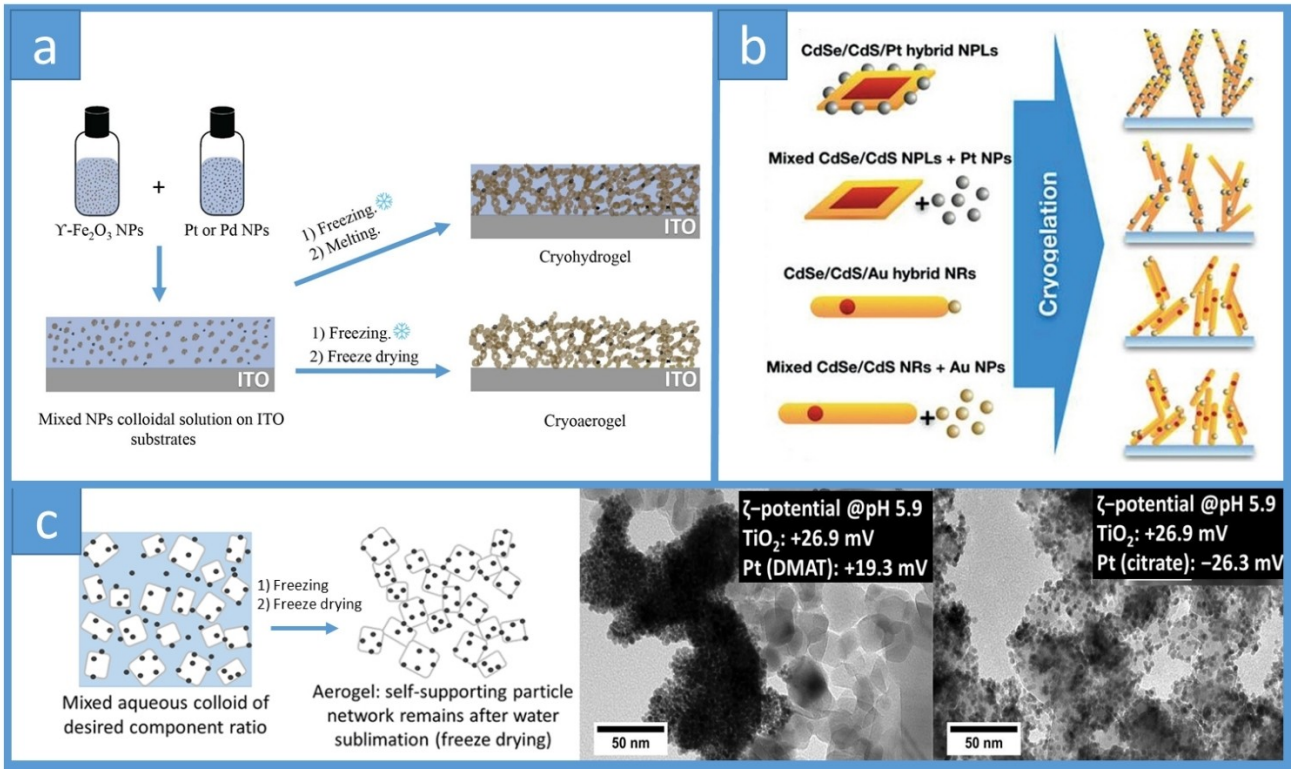

Figure 5. a) Schematic diagram showing the steps for obtaining multicomponent cryoaerogel or cryohydrogel films supported on ITO/glass substrates.[87] Adapted with permission.[87] Copyright 2023 by the authors. License MDPI. b) Schematic diagram showing the different models for obtaining multicomponent cryoaerogels from semiconductor NPLs or NRs combined with noble metal NPs either by mixing the nanoparticles or direct growth of the noble metal domain on the semiconductor.[86] Adapted with permission.[86] Copyright 2022 The Authors. Advanced Materials Interfaces published by Wiley-VCH GmbH. c) Effect of ζ-potentials on the final homogeneity of the cryogel. Right: a diagram showing mixing of the NPs with opposite surface charges resulting in random distribution of the NPs in a homogenous way. Left: TEM images of cryoaerogel monoliths from mixed Pt and TiO_2 NPs with different surface charges, a partial segregation of Pt NPs is observed in the case of the same surface charge for Pt and TiO_2 NPs, a homogenous distribution is observed in the case of opposite surface charges.[21] Adapted with permission.[21] Copyright 2022 American Chemical Society.

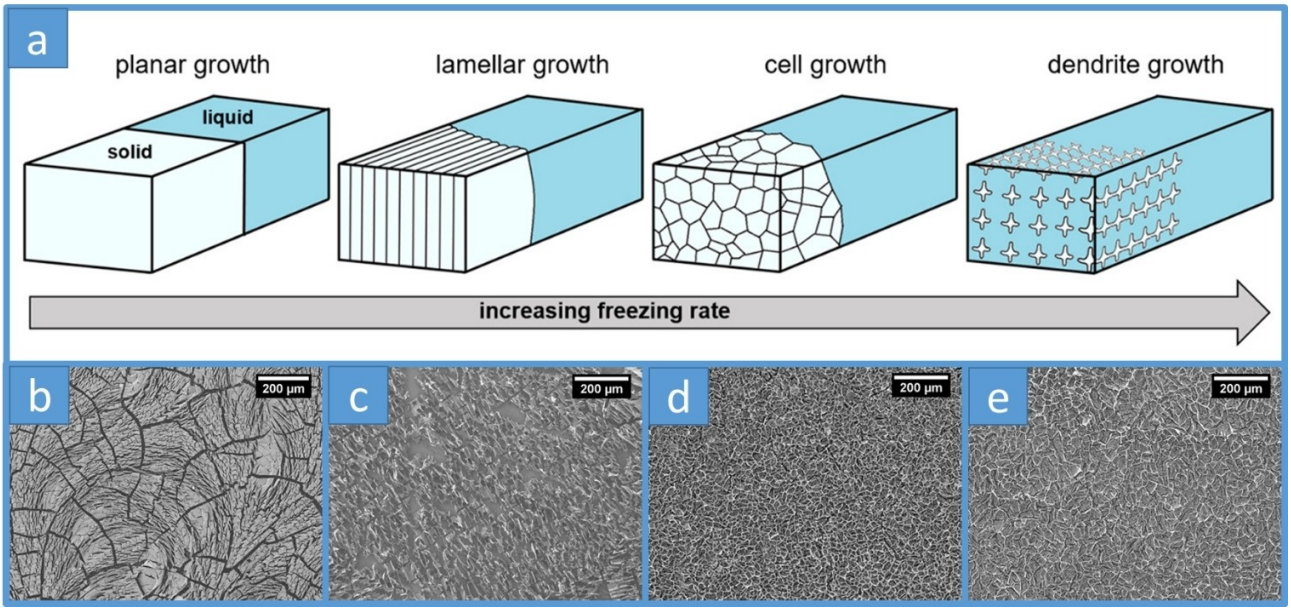

Figure 6. a) The influence of increasing freezing rate on the ice crystal growth, at higher freezing rates small number and size of ice crystals are formed. SEM images of cryoaerogel coatings from Pt NPs resulted from freezing at different temperatures (using different freezing media) b) 235 K (in air atmosphere inside a freezer). c) 77 K using liquid nitrogen. d) 142 K using n-pentane/liquid nitrogen. e) 113 K using isopentane/liquid nitrogen.[14] Adapted with permission.[14] Copyright 2022 The Authors. Published by American Chemical Society.

Table 1. Examples of the different types of NPs used to prepare cryogels and their possible applications.

Type of NPs	Shape of NPs	Size (nm)	Surface ligands	Concentration of colloidal dispersion	Cryogel density	Application/properties investigated	Ref
Au Ag Pt Pd Fe_2O_3 CdSe/CdS nanorods	Spherical except for CdSe/CdS	Au: 3.3 ± 0.4 Ag: 8.6 ± 2.3 Pd: 3.6 ± 0.6 Pt: 3.8 ± 0.7	Citrate MSA TGA	≥ 0.1 % volume fraction	0.02–0.06 g cm^{-1}		[84]
Ag/SiO_2 shell	Spherical	Ag: 68 ± 12 Shell thichness: 5 and 12	PVP	0.3 % Or 29 mg/mL	0.03 g cm^{-1}	Optical properties	[100]
Au + Fe_2O_3 Ag + Fe_2O_3 Ag + TiO_2 Au + TiO_2 Pt + TiO_2 Pt + $MnO(OH)_x$ Pt + $CoO(OH)_x$ Pt + $NiO(OH)_x$	Spherical		Citrate or DMAT for Au, Ag and Pt			Photocatalysis	[21]
CdSe nanoplatelets	Quasi-rectangular	Thickness: 1.2 Length:7.1 ± 1.4 Width: 22.8 ± 2.9	MUA	28 **mM** Cd		Photochemical sensing	[103]
Au	Spherical	4	Citrate	0.1 %		Electrocatalysis	[109]
Au	Nanowires	Length: 10 μm Width: 7 **nm**	Mercaptobenzoic acid (MBA)	2–14 mg/mL	0.006 – 0.023 g cm^{-3}		[111]
Au Pt Pd	Spherical	Au: 4.6 ± 1.2 Pt: 4.6 ± 0.42 Pd:11.2 ± 1.2	Citrate	≥ 0.1 %		Electrocatalysis	[85]
Au Ag	Nanorods	Au: L_{NRs} 46, W_{NRs} 11 Ag: L_{NRs} 108, W_{NRs} 25	Au: CTAB/n-decanol Ag: CTAC	Au^0: 8.8 g/L $Au^0 + Ag^0$: 5.4 g/L		Electrocatalysis	[102]
CdSe/CdS/Pt CdSe/CdS + Pt CdSe/CdS/Au CdSe/CdS + Au	Pt,Au: Spherical CdSe/CdS: Nanoplatelets (NPLs) or Nanorods (NRs)	CdSe/CdS NPLs: L_{NPLs} 54.1 ± 7.1 W_{NPLs} 12.2 ± 1.4 Pt_{domain} 1.9 ± 0.4 Pt_{NPs} 1.7 ± 0.2 CdSe/CdS NRs: L_{NRs} 40.6 ± 5.4 W_{NRs} 4.9 ± 0.5 Au_{domain} 2.7 ± 0.8 Au_{NPs} 4.7 ± 0.7	MUA MPA	0.03–0.07 M		Photoelectrochemical	[86]
Pt + γ-Fe_2O_3 Pd + γ-Fe_2O_3	Spherical	Pt: 3.9 ± 0.2 Pd: 4.4 ± 0.2 γ -Fe_2O_3: 11.3 ± 0.2	Citrate	30–64 g/L		Electrochemical	[87]

cryogel structure formed from pure metal oxides (i.e. hematite)[21] in which the interparticle interaction is relatively weak compared to the intraparticle interaction between the metal ion and the oxygen atoms. This leads to an increased fragility of the cryogel structure due to the higher atomic distances in between the NPs than within the NPs. Another example in which the interparticle distances play an important role is the gel structure made from semiconductor-metal NPs.[86,117] It was found that direct contact between the semiconductor and metal NPs prior to gelation is important for efficient charge carrier separation. In detail, the distribution of the noble metal domain throughout the gel structure can be tuned by direct growth of the metal domains on the semiconductor NPs instead of just mixing the two of them prior to gelation (Figure 5b).

It is very important to note here that the interparticle forces should be carefully modified in order to reduce the repulsive forces in a way that still allow the controlled assembly by further cryogelation. Several approaches are useful to manipulate these interparticle distances, for example, increasing the

metal content or annealing at high temperatures in order to decrease the fragility of the cryogel structure.[21] Additionally, controlling the amount of the residual ligands on the NPs surface to add more cross-linking forces between the NPs is a promising approach.[95] Direct growth of the metal domains on the surface of the semiconductor NPs – as we mentioned earlier – helped to control over the NPs distribution.[86] Finally, mixing NPs of different sizes can also help to decrease the cryogel structure fragility by filling the interparticle spaces with the smaller particles.

4. Applications

Compared to drop casted NPs, the 3D cryogel structure have proven always a better performance in many applications. The unique properties of cryogels made from colloidal NPs represented in the open pores, the high specific surface to volume ratio, the retained nanoscopic properties and many more, as we discussed before. All these characteristics made cryogels excellent candidates for many applications, for example, photocatalysis[21], photoelectrochemical sensing[103] and electrocatalysis.[85,87,102,109,110] In this section we will highlight some examples of the application of cryogels made from NPs with different types, shapes, and sizes.

For electrocatalysis, cryoaerogel and cryohydrogel thin films from pure noble metals NPs (Pt, Pd and Au) supported on ITO substrates were investigated for their electrocatalytic activity to the ethanol oxidation reaction (EOR).[85] The novel materials showed greater electrochemical active surface area (ECSA) and enhancement in the mass activity when compared to the immobilized drop casted NPs on the ITO substrates (Figure 7a). Interestingly, in that work it is shown that the cryogel superstructure is also present in the frozen state after flash-freezing and before the freeze-drying. Cryohydrogels out of noble metal nanoparticles are fabricated by placing the flash-frozen samples in an aqueous solution and left for gentle thawing of the ice crystals, showcasing the same electrocatalytic activity as the re-wetted cryoaerogels which were previously freeze-dried. Another example is cryogel thin films prepared from mixing noble metals NPs (Pt or Pd) with γ-Fe_2O_3 NPs.[87] The cryogel thin films were supported on conductive ITO/glass substrates and investigated for their electrocatalytic activity towards EOR which can be applied in direct alcohol fuel cells. Although the noble metal content was very low (only 1 wt%), however, the cryogel thin films showed better electrocatalytic performance than cryogels from pure noble metal NPs. The mass activity and the ECSA were increased in the case of the multicomponent cryogel structures from mixed Pt or Pd NPs with γ-Fe_2O_3 NPs. Interestingly, the tolerance against the ethanol oxidation reaction intermediates (the poisonous carbon oxide intermediates) was greatly enhanced. Figure 7b compares the cyclic voltammograms obtained from cryohydrogel samples made of pure Pd NPs and 1 wt% Pd/ γ-Fe_2O_3 NPs measured in 0.25 M ethanol at highly basic pH (1 M KOH).

Other study reported the electrocatalytic and photoelectrocatalytic performance of Au–Pt and Au–Pd cryogels for EOR.[94]

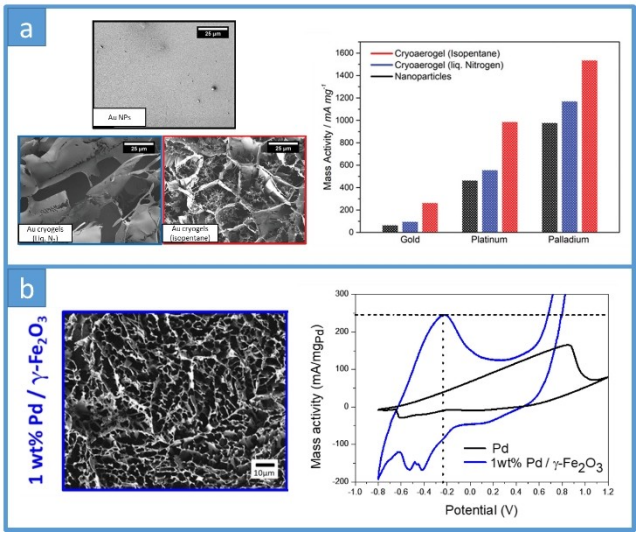

Figure 7. a) Application of cryoaerogel made from pure Au, Pt and Pd in electrocatalytic oxidation of ethanol. Left: SEM images of drop casted Au NPs (black), Au cryoaerogel freezed at −196 °C in liquid nitrogen (blue) and Au cryoaerogel freezed at −160 °C in isopentane/liquid nitrogen (red). Right: The corresponding mass-normalized activities of Au, Pt and Pd coatings for ethanol oxidation reaction.[85] Adapted with permission.[85] Copyright 2021 The Authors. Small published be Wiley-VCH GmbH. b) Application of cryogels made from pure and mixed Pd NPs with γ-Fe_2O_3 NPs in electrocatalytic oxidation of ethanol. Left: SEM image (top view) of cryoaerogel thin film supported on ITO/glass substrate (working electrode), the cryoaerogel is made of mixed Pd and γ-Fe_2O_3 NPs with 1wt% concentration of the noble metal. Right: a comparison between the cyclic voltammograms of: cryohydrogel from pure Pd NPs (black) and cryohydrogel from 1wt% Pd/γ-Fe_2O_3 (blue), scan rate 50 mV/s.[87] Adapted with permission.[87] Copyright 2023 by the authors. License MDPI.

The resulting cryogel benefits from the outstanding properties of both noble metals: the Au provides high stability and electrical conductivity, while the Pt and Pd provide excellent catalytic activities.

Cryogel thin films were prepared from Au and Ag nanorods surface-modified with conductive polymer (poly(3,4-ethylenedioxythiophene) poly(styrenesulfonate) (PEDOT:PSS) and their application in electrocatalysis was studied (Figure 8a).[102] The electrochemical redox reaction was investigated by means of cyclic voltammetry in presence of Cl^- or OH^- ions which revealed the available electrochemical active sites on the cryogelated Au and Ag nanorod surfaces. This work compares the performance of the cryogelated structures with the simply drop casted and dried NPs. The cryogel structures showed very promising results for the electrocatalytic sensing of ferrocyanide, D-glucose and enhanced performance in the catalytic activity towards EOR. The significant decrease in the resistance due to the porous structure of the cryogelated materials was also proved by means of electrochemical impedance spectroscopy in the same study. On the other hand, a study made on porous cryogels from pure Au NPs reported no catalytic activity of these Au cryogels towards carbon monoxide oxidation.[109] However, the same study revealed the importance of trace alkali metals on the Au surfaces and their effect on the catalytic activity of the cryogels. The presence of such trace metals was

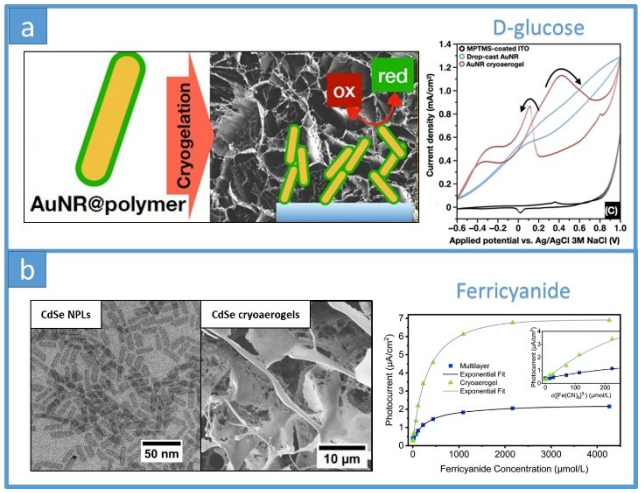

Figure 8. a) Application of cryoaerogels made of Au NRs in electrocatalytic sensing of D-glucose. Left: a diagram shows the assembly of cryoaerogel thin films from Au NRs/PEDOT:PSS on ITO/glass substrate, in the background, an SEM image of a top view of the cryoaerogel thin films. Right: a comparison between the cyclic voltammograms of: bare ITO/glass substrate (black), drop casted Au NRs (blue) and Au NRs cryoaerogel thin film (red).[102] Adapted with permission[102].Copyright 2022 The Authors. Published by American Chemical Society. b) Application of cryoaerogels made of CdSe NPLs. Left: TEM and SEM images of CdSe NPLs and CdSe cryoaerogel coated photoelectrode, respectively. Right: Photocurrent responses Vs ferricyanide concentration measured for a CdSe NPLs deposited as multilayers (blue) and a CdSe NPLs cryoaerogel coated photoelectrode (green).[103] Adapted with permission[103]. Copyright 2019 Royal Society of Chemistry.

found essential for the high catalytic activity of the Au cryogels towards the oxidative methanol coupling.

Cryoaerogels from CdSe nanoplatelets (NPLs) have proven to be very promising in photoelectrochemical sensing applications.[103] The cryoaerogel coated photoelectrode were prepared as thin films supported on functionalized ITO/glass substrates. Compared to drop casted CdSe NPLs, the 3D porous cryoaerogel structure showed higher photocurrent efficiencies up to 6.63 μA/cm^2 and enhanced sensitivity towards ferricyanide down to concentrations less than 5 μM (Figure 8b). The improvement in the photoelectrochemical performance is attributed to the better charge carrier mobility in the case of the highly porous structure of the cryoaerogels. For photocatalysis, cryoaerogels prepared from mixed Pt and TiO_2 NPs were evaluated for their photocatalytic activity towards Hydrogel evolution reaction.[21] In this work, the composition of the cryoaerogel structure was fine-tuned by controlling the ratio of Pt to TiO_2. This was done by simply mixing the two types of the NPs with different amounts (1, 50 and 84 wt% of Pt). It was proven that the Pt content play very important role in the photocatalytic performance of the cryoaerogels for hydrogen evolution reaction as well as for the stability of the cryoaerogel structure. The cryoaerogel with 1 wt% Pt showed the highest photocatalytic activity, with an average specific hydrogen evolution of 5.1 mmol h^{-1} g^{-1}. Interestingly, this value is higher than the obtained for the 1 wt% Pt colloidal solution (3.1 mmol h^{-1} g^{-1}). As well, this work proves that cryoaerogels have better photocatalytic performance compared to the highest value of hydrogen evolution by aerogels prepared by conventional hydrogelation methods.

5. Summary and Outlook

Nanocrystal-based cryogels are highly promising novel materials showcasing high surface areas and a porous structure which bridge the gap between the macroscopic scale and the nanoscopic properties of the building blocks. The huge library of options for these building blocks, either regarding on their composition (semiconducting, magnetic, plasmonic or mixtures of them[86]), their size and shape (nanowires[26,112,118], nanoplatelets[103,119], spheres, cubes …) or their surface functionalization, open the possibility to tackle a broad range of societal problems, such as environmental remediation[25,55,120] or energy saving and conversion.[15,121] Their superior performance in several applications such as electro- or photocatalysis in comparison to the colloidal counterpart has been extensively proven,[21,85,87,110] being possible to obtain better catalysts with lower loads of noble metals, which decrease considerably the price and overcome the problem of the scarcity of these elements. This is possible because these materials maximize the available active surface area, improving the catalytic mass activity. In addition, the fabrication of cryogels directly out of the aqueous colloidal solution of inorganic nanoparticles is extremely easy and very versatile, not being necessary any previous milling or hydrogelation, and it is possible to obtain thin films as well as sponge-like monoliths which can be molded as desired. As they are self-supported, no co-catalyst or support is necessary, so the long-time stability against (electro-)corrosion is improved compared to the commercially available materials based on carbon,[122] and the heat transfer is increased.

The applications found in literature regarding nano-crystal-based cryogel are limited to a few examples, while the potential and possibilities of these materials are broad, due to the enormous toolbox of inorganic nanocrystals available nowadays. Especially due to the possibility of external shaping e.g. by doctor blading, the processability and hence applicability of these materials might possibly be even higher than in conventionally synthesized gels. In this context, the application of these materials can be expanded to include: all kind of catalysis (e.g., water electrolysis, gas-phase catalysis and photocatalysis), biomedical applications for diagnostics and analysis (e.g., analysis of pharmaceuticals and bioactive molecules), environmental applications (e.g., adsorbent in water treatment), and last but not least, in the field of electronics as insulators, conductors, supercapacitors or further high-surface electrodes.[1,123–127]

Nevertheless, there are still different challenges to overcome to exploit the full potential of these materials. Cryogels made out only by inorganic nanocrystals are very brittle and fragile, and more research should be done in the direction of increasing their thermal, mechanical and catalytic stability, in particular the long-term catalytic stability over multiple runs. For the latter, for example, it has been found that while Ag, Au

and Pt cryogel catalysts (for CO oxidation) exhibit a decreased thermal stability and catalytic activity over several runs, Pd cryogel exhibits significantly high stability.[110] By the correct choice of the catalytic material, the temperature and freezing rate and surface functionalization, it is possible to increase the catalytic activity. In the sense of mechanical stability, all nanocrystal-based gels are fragile, whether obtained by conventional gelation or cryogelation. It might be that due to the side-by-side connection of the nanoparticles there could be higher stability, but it has not yet been measured to the best of our knowledge. There is a lot of research done in the direction of mixing inorganic nanoparticles with polymer matrices, which considerably diminishes their fragility.[26,118,128] It was also suggested that the quality of the NPs dispersion and optimization of the gelation step can enhance the mechanical stability of nanocrystal-based aerogels. Additionally, a high homogeneity of the gel components over the entire gel volume is crucial to improve the mechanical stability.[95]

Finally, for the fabrication of cryogel thin films on conductive substrates, it is very important to focus on the correct functionalization of the nanoparticles and the substrate, to secure a good attachment of the cryogel and therefore a better and higher stability catalyst.[102]

The interest on studying nanocrystal-based cryogels is clear from different point of views: i) the easy synthesis procedure, ii) their lightness, porous structure and enhanced surface area, iii) their outstanding performance in different catalytic applications and iv) the possibility of reducing the load of noble metal in the catalyst, reducing the overall cost. Using novel or modified cryogelation techniques, as for example cryoprinting, tailored and improved cryogels will be obtained with the desired functionalities and new potential applications by the correct choice of the building blocks.

Acknowledgements

This work has received funding from the Deutsche Forschungsgemeinschaft (DFG, German Research Foundation) under Germany's Excellence Strategy within the Cluster of Excellence PhoenixD (EXC 2122, Project ID 390833453) and the Cluster of Excellence CUI: Advanced Imaging of Matter' (EXC2056, project ID 390715994). We acknowledge financial support from the Open Access Publication Fund of Universität Hamburg. I.M. thanks the Leibniz Universität Hannover and the Cluster of Excellence PhoenixD for funding within the Caroline Herschel Programme. Furthermore, N.C.B. thanks the DFG (Research Grant BI 1708/4-3) for funding. Open Access funding enabled and organized by Projekt DEAL.

Conflict of Interests

The authors declare no conflict of interest.

Keywords: cryogels · freeze-drying · nanocrystal building blocks · catalysis

[1] C. Ziegler, A. Wolf, W. Liu, A.-K. Herrmann, N. Gaponik, A. Eychmüller, *Angew. Chem. Int. Ed.* **2017**, *56*, 13200–13221.
[2] A. M. Green, C. K. Ofosu, J. Kang, E. V. Anslyn, T. M. Truskett, D. J. Milliron, *Nano Lett.* **2022**, *22*, 1457–1466.
[3] P. Rusch, D. Zámbó, N. C. Bigall, *Acc. Chem. Res.* **2020**, *53*, 2414–2424.
[4] M. Niederberger, in *Springer Handb. Aerogels* (Eds.: M. A. Aegerter, N. Leventis, M. Koebel, S. A. Steiner III), Springer International Publishing, Cham, **2023**, pp. 1041–1060.
[5] D. Müller, D. Wen, A. Eychmüller, N. C. Bigall, in *Springer Handb. Aerogels* (Eds.: M. A. Aegerter, N. Leventis, M. Koebel, S. A. Steiner III), Springer International Publishing, Cham, **2023**, pp. 1061–1087.
[6] F. J. Burpo, in *Springer Handb. Aerogels* (Eds.: M. A. Aegerter, N. Leventis, M. Koebel, S. A. Steiner III), Springer International Publishing, Cham, **2023**, pp. 1089–1127.
[7] F. Lübkemann-Warwas, I. Morales, N. C. Bigall, *Small Struct.* **n.d.**, 2300062.
[8] M. A. Boles, M. Engel, D. V. Talapin, *Chem. Rev.* **2016**, *116*, 11220–11289.
[9] J. V. Alemán, A. V. Chadwick, J. He, M. Hess, K. Horie, R. G. Jones, P. Kratochvíl, I. Meisel, I. Mita, G. Moad, S. Penczek, R. F. T. Stepto, *Pure Appl. Chem.* **2007**, *79*, 1801–1829.
[10] M. E. El-Naggar, S. I. Othman, A. A. Allam, O. M. Morsy, *Int. J. Biol. Macromol.* **2020**, *145*, 1115–1128.
[11] S. S. Kistler, *Nature* **1931**, *127*, 741–741.
[12] P. H. Tewari, A. J. Hunt, K. D. Lofftus, *Mater. Lett.* **1985**, *3*, 363–367.
[13] A. Kumar, R. Mishra, Y. Reinwald, S. Bhat, *Mater. Today* **2010**, *13*, 42–44.
[14] D. Müller, L. F. Klepzig, A. Schlosser, D. Dorfs, N. C. Bigall, *Langmuir* **2021**, *37*, 5109–5117.
[15] O. A. Shlyakhtin, Y.-J. Oh, *J. Electroceram.* **2008**, *23*, 452.
[16] A. Memic, T. Colombani, L. J. Eggermont, M. Rezaeeyazdi, J. Steingold, Z. J. Rogers, K. J. Navare, H. S. Mohammed, S. A. Bencherif, *Adv. Ther.* **2019**, *2*, 1800114.
[17] V. I. Lozinsky, in *Polym. Cryogels Macroporous Gels Remarkable Prop.* (Ed.: O. Okay), Springer International Publishing, Cham, **2014**, pp. 1–48.
[18] L. Hossain, V. S. Raghuwanshi, J. Tanner, G. Garnier, *Colloids Surf. Physicochem. Eng. Asp.* **2021**, *630*, 127608.
[19] R. Rodríguez-Dorado, C. López-Iglesias, C. A. García-González, G. Auriemma, R. P. Aquino, P. Del Gaudio, *Molecules* **2019**, *24*, 1049.
[20] I. V. Tyshkunova, D. N. Poshina, Y. A. Skorik, *Int. J. Mol. Sci.* **2022**, *23*, 2037.
[21] A. Freytag, C. Günnemann, S. Naskar, S. Hamid, F. Lübkemann, D. Bahnemann, N. C. Bigall, *ACS Appl. Nano Mater.* **2018**, *1*, 6123–6130.
[22] M. Bakhshpour, N. Idil, I. Perçin, A. Denizli, *Appl. Sci.* **2019**, *9*, 553.
[23] A. M. Mohammed, K. T. Hassan, O. M. Hassan, *Int. J. Biol. Macromol.* **2023**, *233*, 123580.
[24] A. Haleem, S.-Q. Chen, M. Ullah, M. Siddiq, W.-D. He, *J. Environ. Chem. Eng.* **2021**, *9*, 106510.
[25] A. Mohammadi, A. Mirzaei, S. Javanshir, *RSC Adv.* n.d., *12*, 16215–16228.
[26] S. M. Jung, D. J. Preston, H. Y. Jung, Z. Deng, E. N. Wang, J. Kong, *Adv. Mater.* **2016**, *28*, 1413–1419.
[27] A. K. Nayak, B. Das, in *Polym. Gels* (Eds.: K. Pal, I. Banerjee), Woodhead Publishing, **2018**, pp. 3–27.
[28] T. M. A. Henderson, K. Ladewig, D. N. Haylock, K. M. McLean, A. J. O'Connor, *J. Mater. Chem. B* **2013**, *1*, 2682–2695.
[29] L. Boulais, R. Jellali, U. Pereira, E. Leclerc, S. A. Bencherif, C. Legallais, *ACS Appl. Bio Mater.* **2021**, *4*, 5617–5626.
[30] A. Wartenberg, J. Weisser, M. Schnabelrauch, *Molecules* **2021**, *26*, 5597.
[31] S. S. Suner, S. Demirci, B. Yetiskin, R. Fakhrullin, E. Naumenko, O. Okay, R. S. Ayyala, N. Sahiner, *Int. J. Biol. Macromol.* **2019**, *130*, 627–635.
[32] H. Omidian, S. Dey Chowdhury, N. Babanejad, *Pharmaceutica* **2023**, *15*, 1836.
[33] K. R. Hixon, T. Lu, S. A. Sell, *Acta Biomater.* **2017**, *62*, 29–41.
[34] N. Xu, Y. Yuan, L. Ding, J. Li, J. Jia, Z. Li, D. He, Y. Yu, *Burns Trauma* **2022**, *10*, tkac019.
[35] E. K. Radwan, M. E. El-Naggar, A. Abdel-Karim, A. R. Wassel, *Int. J. Biol. Macromol.* **2021**, *189*, 420–431.
[36] M. E. El-Naggar, M. Hasanin, A. M. Youssef, A. Aldalbahi, M. H. El-Newehy, R. M. Abdelhameed, *Int. J. Biol. Macromol.* **2020**, *165*, 1010–1021.

[37] A. M. Abdelgawad, M. E. El-Naggar, D. A. Elsherbiny, S. Ali, M. S. Abdel-Aziz, Y. K. Abdel-Monem, *J. Environ. Chem. Eng.* **2020**, *8*, 104276.
[38] T. Zhao, S. Zhang, Y. Bi, D. Sun, F. Kong, Z. Yuan, X. Xin, *Colloids Surf. Physicochem. Eng. Asp.* **2020**, *603*, 125257.
[39] K. Erol, M. Bolat, D. Tatar, C. Nigiz, D. A. Köse, *J. Mol. Struct.* **2020**, *1200*, 127060.
[40] D. Demir, S. Özdemir, M. S. Yalçın, N. Bölgen, *Int. J. Polym. Mater.* **2020**, *69*, 919–927.
[41] M. Fan, L. Gong, Y. Huang, D. Wang, Z. Gong, *Sci. Total Environ.* **2018**, *613–614*, 1317–1323.
[42] X. Zou, P. Deng, C. Zhou, Y. Hou, R. Chen, F. Liang, L. Liao, *J. Biomater. Sci. Polym. Ed.* **2017**, *28*, 1324–1337.
[43] S.-L. Loo, W. B. Krantz, X. Hu, A. G. Fane, T.-T. Lim, *J. Colloid Interface Sci.* **2016**, *461*, 104–113.
[44] S.-L. Loo, W. B. Krantz, A. G. Fane, Y. Gao, T.-T. Lim, X. Hu, *Environ. Sci. Technol.* **2015**, *49*, 2310–2318.
[45] S.-L. Loo, W. B. Krantz, A. G. Fane, X. Hu, T.-T. Lim, *RSC Adv.* **2015**, *5*, 44626–44635.
[46] S.-L. Loo, A. G. Fane, T.-T. Lim, W. B. Krantz, Y.-N. Liang, X. Liu, X. Hu, *Environ. Sci. Technol.* **2013**, *47*, 9363–9371.
[47] F. Zhang, J. Wu, D. Kang, H. Zhang, *J. Biomater. Sci. Polym. Ed.* **2013**, *24*, 1410–1425.
[48] N. Nontipichet, S. Khumngern, J. Choosang, P. Thavarungkul, P. Kanatharana, A. Numnuam, *Food Chem.* **2021**, *364*, 130396.
[49] J. Choosang, S. Khumngern, P. Thavarungkul, P. Kanatharana, A. Numnuam, *Talanta* **2021**, *224*, 121787.
[50] S. Singh, A. Gupta, I. Qayoom, A. K. Teotia, S. Gupta, P. Padmanabhan, A. Dev, A. Kumar, *J. Nanopart. Res.* **2020**, *22*, 152.
[51] D. Berillo, *J. Cleaner Prod.* **2020**, *247*, 119089.
[52] T. Kangkamano, A. Numnuam, W. Limbut, P. Kanatharana, P. Thavarungkul, *Sens. Actuators B* **2017**, *246*, 854–863.
[53] S. Samanman, A. Numnuam, W. Limbut, P. Kanatharana, P. Thavarungkul, *Anal. Chim. Acta* **2015**, *853*, 521–532.
[54] D. Berillo, B. Mattiasson, H. Kirsebom, *Biomacromolecules* **2014**, *15*, 2246–2255.
[55] D. A. Berillo, I. N. Savina, *Inorganics* **2023**, *11*, 23.
[56] D. Berillo, A. Cundy, *Carbohydr. Polym.* **2018**, *192*, 166–175.
[57] S. Demirci, N. Sahiner, *ChemCatChem* **2023**, *15*, e202201498.
[58] M. Tercan, S. Demirci, O. Dayan, N. Sahiner, *New J. Chem.* **2020**, *44*, 4417–4425.
[59] N. Sahiner, S. Yildiz, M. Sahiner, Z. A. Issa, H. Al-Lohedan, *Appl. Surf. Sci.* **2015**, *354*, 388–396.
[60] N. Sahiner, S. Yildiz, H. Al-Lohedan, *Appl. Catal. B* **2015**, *166–167*, 145–154.
[61] N. Sahiner, S. Yildiz, *Fuel Process. Technol.* **2014**, *126*, 324–331.
[62] S. Yildiz, N. Aktas, N. Sahiner, *Int. J. Hydrogen Energy* **2014**, *39*, 14690–14700.
[63] N. Sahiner, F. Seven, *Energy* **2014**, *71*, 170–179.
[64] "Simultaneous degradation and reduction of multiple organic compounds by poly(vinyl imidazole) cryogel-templated Co, Ni, and Cu metal nanoparticles - New Journal of Chemistry (RSC Publishing)," can be found under https://pubs.rsc.org/en/content/articlelanding/2020/nj/d0nj00148a, n.d.
[65] T. I. Shabatina, O. I. Vernaya, A. V. Nuzhdina, V. P. Shabatin, A. M. Semenov, M. Ya. Mel'nikov, *Russ. J. Phys. Chem. A* **2019**, *93*, 1970–1975.
[66] E. I. Anastasova, A. A. Belyaeva, S. A. Tsymbal, D. A. Vinnik, V. V. Vinogradov, *J. Colloid Interface Sci.* **2022**, *615*, 206–214.
[67] F. Wang, R. Ma, J. Zhan, W. Shi, Y. Zhu, Y. Tian, *Sep. Purif. Technol.* **2022**, *291*, 120872.
[68] K. Çetin, *Process Biochem.* **2022**, *112*, 203–208.
[69] S. Teepoo, T. Laochai, *Anal. Lett.* **2022**, *55*, 828–840.
[70] T. Laochai, M. Mooltongchun, S. Teepoo, *Energy Procedia* **2016**, *89*, 248–254.
[71] K. Yao, S. Shen, J. Yun, L. Wang, F. Chen, X. Yu, *Biochem. Eng. J.* **2007**, *36*, 139–146.
[72] S. A. El-Kholy, E. K. Radwan, M. E. El-Naggar, S. T. El-Wakeel, I. El-Tantawy El Sayed, *J. Environ. Chem. Eng.* **2023**, *11*, 110652.
[73] M. E. El-Naggar, S. Gaballah, G. Abdel-Maksoud, H. S. El-Sayed, A. M. Youssef, *J. Mater. Res.* **2022**, *20*, 114–127.
[74] P. Xu, Y. Yao, S. Shen, J. Yun, K. Yao, *Chin. J. Chem. Eng.* **2010**, *18*, 667–671.
[75] L. Önnby, V. Pakade, B. Mattiasson, H. Kirsebom, *Water Res.* **2012**, *46*, 4111–4120.
[76] M. Zhang, Y. Li, E. Uchaker, S. Candelaria, L. Shen, T. Wang, G. Cao, *Nano Energy* **2013**, *2*, 769–778.
[77] A. Baimenov, D. A. Berillo, S. G. Poulopoulos, V. J. Inglezakis, *Adv. Colloid Interface Sci.* **2020**, *276*, 102088.
[78] L. Wang, J. Jiang, W. Hua, A. Darabi, X. Song, C. Song, W. Zhong, M. M. Q. Xing, X. Qiu, *Adv. Funct. Mater.* **2016**, *26*, 4293–4305.
[79] Z. Deng, Y. Guo, P. X. Ma, B. Guo, *J. Colloid Interface Sci.* **2018**, *526*, 281–294.
[80] Y. Liu, K. Xu, Q. Chang, M. A. Darabi, B. Lin, W. Zhong, M. Xing, *Adv. Mater.* **2016**, *28*, 7758–7767.
[81] C. Yang, Y. Zhang, W.-Q. Cao, Y.-N. Yan, J. Wang, X.-F. Ji, T.-L. Zhong, Y. Wang, *J. Fluoresc.* **2018**, *28*, 337–345.
[82] O. Okay, Ed., *Polymeric Cryogels: Macroporous Gels with Remarkable Properties*, Springer International Publishing, Cham, **2014**.
[83] H.-L. Gao, L. Xu, F. Long, Z. Pan, Y.-X. Du, Y. Lu, J. Ge, S.-H. Yu, *Angew. Chem. Int. Ed.* **2014**, *53*, 4561–4566.
[84] A. Freytag, S. Sánchez-Paradinas, S. Naskar, N. Wendt, M. Colombo, G. Pugliese, J. Poppe, C. Demirci, I. Kretschmer, D. W. Bahnemann, P. Behrens, N. C. Bigall, *Angew. Chem. Int. Ed. Engl.* **2016**, *55*, 1200–1203.
[85] D. Müller, D. Zámbó, D. Dorfs, N. C. Bigall, *Small* **2021**, *17*, 2007908.
[86] A. Schlosser, J. Schlenkrich, D. Zámbó, M. Rosebrock, R. T. Graf, G. Escobar Cano, N. C. Bigall, *Adv. Mater. Interfaces* **2022**, *9*, 2200055.
[87] H. Borg, I. Morales, D. Kranz, N. C. Bigall, D. Dorfs, *Catalysts* **2023**, *13*, 1074.
[88] P. Arvidsson, F. M. Plieva, V. I. Lozinsky, I. Y. Galaev, B. Mattiasson, *J. Chromatogr. A* **2003**, *986*, 275–290.
[89] A. Tripathi, A. Kumar, *Macromol. Biosci.* **2011**, *11*, 22–35.
[90] P. Arvidsson, F. M. Plieva, I. N. Savina, V. I. Lozinsky, S. Fexby, L. Bülow, I. Yu. Galaev, B. Mattiasson, *J. Chromatogr. A* **2002**, *977*, 27–38.
[91] S. Asliyuce, L. Uzun, A. Yousefi Rad, S. Unal, R. Say, A. Denizli, *J. Chromatogr. B* **2012**, *889–890*, 95–102.
[92] F. M. Plieva, B. Mattiasson, *Ind. Eng. Chem. Res.* **2008**, *47*, 4131–4141.
[93] R. Du, Y. Hu, R. Hübner, J.-O. Joswig, X. Fan, K. Schneider, A. Eychmüller, *Sci. Adv.* **2019**, *5*, eaaw4590.
[94] R. Du, J.-O. Joswig, R. Hübner, L. Zhou, W. Wei, Y. Hu, A. Eychmüller, *Angew. Chem. Int. Ed.* **2020**, *59*, 8293–8300.
[95] F. Matter, A. L. Luna, M. Niederberger, *Nano Today* **2020**, *30*, 100827.
[96] A. Eychmüller, *J. Phys. Chem. C* **2022**, *126*, 19011–19023.
[97] H. Wang, Q. Fang, W. Gu, D. Du, Y. Lin, C. Zhu, *ACS Appl. Mater. Interfaces* **2020**, *12*, 52234–52250.
[98] F. Rechberger, M. Niederberger, *Nanoscale Horiz.* **2016**, *2*, 6–30.
[99] I. U. Arachchige, S. L. Brock, *Acc. Chem. Res.* **2007**, *40*, 801–809.
[100] T. Kodanek, A. Freytag, A. Schlosser, S. Naskar, T. Härtling, D. Dorfs, N. C. Bigall, *Zeitschrift für Phys. Chemie* **2018**, *232*, 1675–1689.
[101] D. Frederichi, M. H. N. O. Scaliante, R. Bergamasco, *Environ. Sci. Pollut. Res. Int.* **2021**, *28*, 23610–23633.
[102] D. Zámbó, P. Rusch, F. Lübkemann, N. C. Bigall, *ACS Appl. Mater. Interfaces* **2021**, *13*, 57774–57785.
[103] A. Schlosser, L. C. Meyer, F. Lübkemann, J. F. Miethe, N. C. Bigall, *Phys. Chem. Chem. Phys.* **2019**, *21*, 9002–9012.
[104] Y. Wang, X. Zhou, S. Zhu, X. Wei, N. Zhou, X. Liao, Y. Peng, Y. Tang, L. Zhang, X. Yang, Y. Li, X. Xu, J. Tao, R. Liu, *Mater. Des.* **2022**, *223*, 111120.
[105] T.-C. Chen, C.-W. Wong, S. Hsu, *Carbohydr. Polym.* **2022**, *285*, 119228.
[106] Ç. Bilici, M. Altunbek, F. Afghah, A. G. Tatar, B. Koç, *ACS Biomater. Sci. Eng.* **2023**, *9*, 5028–5038.
[107] F. Lübkemann, J. F. Miethe, F. Steinbach, P. Rusch, A. Schlosser, D. Zámbó, T. Heinemeyer, D. Natke, D. Zok, D. Dorfs, N. C. Bigall, *Small* **2019**, *15*, 1902186.
[108] X. Wu, L. Black, G. Santacana-Laffitte, C. W. Patrick Jr., *J. Biomed. Mater. Res. Part A* **2007**, *81 A*, 59–65.
[109] C. Demirci, S. Marras, M. Prato, L. Pasquale, L. Manna, M. Colombo, *J. Catal.* **2019**, *375*, 279–286.
[110] A. Freytag, M. Colombo, N. C. Bigall, *Zeitschrift für Phys. Chemie* **2017**, *231*, 63–75.
[111] F. Qian, A. Troksa, T. M. Fears, M. H. Nielsen, A. J. Nelson, T. F. Baumann, S. O. Kucheyev, T. Y.-J. Han, M. Bagge-Hansen, *Nano Lett.* **2020**, *20*, 131–135.
[112] H.-L. Gao, L. Xu, F. Long, Z. Pan, Y.-X. Du, Y. Lu, J. Ge, S.-H. Yu, *Angew. Chem. Int. Ed.* **2014**, *53*, 4561–4566.
[113] A. M. Abdelmonem, D. Zámbó, P. Rusch, A. Schlosser, L. F. Klepzig, N. C. Bigall, *Macromol. Rapid Commun.* **2022**, *43*, 2100794.
[114] J. L. Mohanan, I. U. Arachchige, S. L. Brock, *Science* **2005**, *307*, 397–400.
[115] T. Berestok, P. Guardia, S. Estradé, J. Llorca, F. Peiró, A. Cabot, S. L. Brock, *Nanomaterials* **2018**, *8*, 220.

[116] N. C. Bigall, A.-K. Herrmann, M. Vogel, M. Rose, P. Simon, W. Carrillo-Cabrera, D. Dorfs, S. Kaskel, N. Gaponik, A. Eychmüller, *Angew. Chem. Int. Ed.* **2009**, *48*, 9731–9734.
[117] J. Schlenkrich, D. Zámbó, A. Schlosser, P. Rusch, N. C. Bigall, *Adv. Opt. Mater.* **2022**, *10*, 2101712.
[118] F. Qian, P. C. Lan, M. C. Freyman, W. Chen, T. Kou, T. Y. Olson, C. Zhu, M. A. Worsley, E. B. Duoss, C. M. Spadaccini, T. Baumann, T. Y.-J. Han, *Nano Lett.* **2017**, *17*, 7171–7176.
[119] R. T. Graf, A. Schlosser, D. Zámbó, J. Schlenkrich, P. Rusch, A. Chatterjee, H. Pfnür, N. C. Bigall, *Adv. Funct. Mater.* **2022**, *32*, 2112621.
[120] L. Otero-González, S. V. Mikhalovsky, M. Václavíková, M. V. Trenikhin, A. B. Cundy, I. N. Savina, *J. Hazard. Mater.* **2020**, *381*, 120996.
[121] J. Zhu, R. Xiong, F. Zhao, T. Peng, J. Hu, L. Xie, H. Xie, K. Wang, C. Jiang, *ACS Sustainable Chem. Eng.* **2020**, *8*, 71–83.
[122] M. Georgi, B. Klemmed, A. Benad, A. Eychmüller, *Mater. Chem. Front.* **2019**, *3*, 1586–1592.
[123] T. Wang, D. Zhang, J. Fei, W. Yu, J. Zhu, Y. Zhang, Y. Shi, M. Tian, J. Lai, L. Wang, *Appl. Catal. B* **2024**, *343*, 123546.
[124] J. E. Amonette, J. Matyáš, *Microporous Mesoporous Mater.* **2017**, *250*, 100–119.
[125] S. Karamikamkar, E. P. Yalcintas, R. Haghniaz, N. R. de Barros, M. Mecwan, R. Nasiri, E. Davoodi, F. Nasrollahi, A. Erdem, H. Kang, J. Lee, Y. Zhu, S. Ahadian, V. Jucaud, H. Maleki, M. R. Dokmeci, H.-J. Kim, A. Khademhosseini, *Adv. Sci.* **2023**, *10*, 2204681.
[126] I. Smirnova, C. A. García-González, P. Gurikov, in *Springer Handb. Aerogels* (Eds.: M. A. Aegerter, N. Leventis, M. Koebel, S. A. Steiner III), Springer International Publishing, Cham, **2023**, pp. 1489–1504.
[127] M. T. Noman, N. Amor, A. Ali, S. Petrik, R. Coufal, K. Adach, M. Fijalkowski, *Gels* **2021**, *7*, 264.
[128] Y. Tang, S. Gong, Y. Chen, L. W. Yap, W. Cheng, *ACS Nano* **2014**, *8*, 5707–5714.

Manuscript received: November 3, 2023
Revised manuscript received: February 14, 2024
Accepted manuscript online: February 26, 2024
Version of record online: March 14, 2024